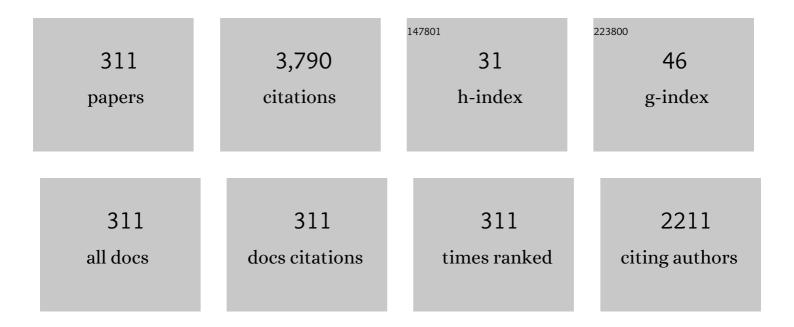
List of Publications by Year in descending order

Source: https://exaly.com/author-pdf/7414780/publications.pdf Version: 2024-02-01



Επιτί Χτι

#	Article	IF	CITATIONS
1	An Eddy Current Testing Method for Thickness and Conductivity Measurement of Non-Magnetic Material. IEEE Sensors Journal, 2023, 23, 4445-4454.	4.7	7
2	Conductivity estimation of non-magnetic materials using eddy current method. Nondestructive Testing and Evaluation, 2023, 38, 130-146.	2.1	11
3	A Robust Deconvolution Method of Airborne LiDAR Waveforms for Dense Point Clouds Generation in Forest. IEEE Transactions on Geoscience and Remote Sensing, 2022, 60, 1-14.	6.3	4
4	Recent progress on laser absorption spectroscopy for determination of gaseous chemical species. Applied Spectroscopy Reviews, 2022, 57, 112-152.	6.7	40
5	A Modified Adaptive Cross Correlation Method for Flow Rate Measurement of High-Water-Cut Oil-Water Flow Using Planar Flowmeter. IEEE Transactions on Instrumentation and Measurement, 2022, 71, 1-10.	4.7	3
6	Development of a Wearable Gesture Recognition System Based on Two-Terminal Electrical Impedance Tomography. IEEE Journal of Biomedical and Health Informatics, 2022, 26, 2515-2523.	6.3	10
7	A Modified Noise Model of Electrical Impedance Tomography System by Considering Colored Noises. IEEE Transactions on Instrumentation and Measurement, 2022, 71, 1-10.	4.7	6
8	Time-Division-Multiplexed Online Gauss-Newton-Based Multi-Echo Decomposition Method for Real-Time <i>In-Situ</i> Laser Ranging. IEEE Sensors Journal, 2022, 22, 4152-4163.	4.7	1
9	A Fabry–Perot Fiber-Optic Array for Photoacoustic Imaging. IEEE Transactions on Instrumentation and Measurement, 2022, 71, 1-8.	4.7	7
10	B-Spline Based Progressive Decomposition of LiDAR Waveform With Low SNR. IEEE Transactions on Instrumentation and Measurement, 2022, 71, 1-12.	4.7	3
11	Sparse Zernike Fitting for Dynamic LAS Tomographic Images of Temperature and Water Vapor Concentration. IEEE Transactions on Instrumentation and Measurement, 2022, 71, 1-14.	4.7	7
12	Direct image reconstruction in electrical tomography and its applications. , 2022, , 389-425.		0
13	Functionalized Macrophage Exosomes with Panobinostat and PPM1Dâ€siRNA for Diffuse Intrinsic Pontine Cliomas Therapy. Advanced Science, 2022, 9, e2200353.	11.2	29
14	Multienzyme System in Amorphous Metal–Organic Frameworks for Intracellular Lactate Detection. Nano Letters, 2022, 22, 5029-5036.	9.1	37
15	A Novel Conductivity Measurement Method for Non-Magnetic Materials Based on Sweep-Frequency Eddy Current Method. IEEE Transactions on Instrumentation and Measurement, 2022, 71, 1-12.	4.7	14
16	A fast reconstruction strategy to image small objects in electrical tomography. , 2022, , .		1
17	A Interferometer modulated TDLAS Temperature Sensor by using Coherent Demodulation. , 2022, , .		1
18	Temperature Telemetry with Synchronous Distance Detection System based on CM-TDLAS. , 2022, , .		0

#	Article	IF	CITATIONS
19	Optimization of 3-D Sensor Design for Electrical Capacitance Tomography. , 2022, , .		1
20	Measurement of tube thickness using eddy current testing based on the modified integration range. , 2022, , .		0
21	Optical ultrasound sensing for biomedical imaging. Measurement: Journal of the International Measurement Confederation, 2022, 200, 111620.	5.0	2
22	Damped Gauss-Newton based online ranging for point extraction from low SNR and high overlapping waveforms. Measurement: Journal of the International Measurement Confederation, 2022, 199, 111479.	5.0	9
23	Simultaneous Shape and Permittivity Reconstruction in ECT With Sparse Representation: Two-Phase Distribution Imaging. IEEE Transactions on Instrumentation and Measurement, 2021, 70, 1-14.	4.7	18
24	Real-Time <i>In-Situ</i> Laser Ranging via Back Propagation Neural Network on FPGA. IEEE Sensors Journal, 2021, 21, 4664-4673.	4.7	6
25	Deep Image Refinement Method by Hybrid Training With Images of Varied Quality in Electrical Capacitance Tomography. IEEE Sensors Journal, 2021, 21, 6342-6355.	4.7	12
26	Super-Resolution Ultrasound Lamb Wave NDE Imaging of Anisotropic Airplane Laminates via Deconvolutional Neural Network. IEEE Transactions on Instrumentation and Measurement, 2021, 70, 1-8.	4.7	5
27	Image Reconstruction Based on Fuzzy Adaptive Kalman Filter in Electrical Capacitance Tomography. IEEE Transactions on Instrumentation and Measurement, 2021, 70, 1-10.	4.7	5
28	A Concurrent Plantar Stress Sensing and Energy Harvesting Technique by Piezoelectric Insole Device and Rectifying Circuitry. IEEE Sensors Journal, 2021, 21, 26364-26372.	4.7	8
29	A Piezoelectric Force Sensing and Gesture Monitoring-Based Technique for Acupuncture Quantification. IEEE Sensors Journal, 2021, 21, 26337-26344.	4.7	4
30	Noise Immune TDLAS Temperature Measurement Through Spectrum Shifting by Using a Mach–Zehnder Interferometer. IEEE Transactions on Instrumentation and Measurement, 2021, 70, 1-9.	4.7	9
31	Revised Calderon Method of Annular ECT for Imaging Flashback Flame of a Bluff-Body Burner. IEEE Transactions on Instrumentation and Measurement, 2021, 70, 1-10.	4.7	3
32	A Machine-Learning-Based Touch Orientation Detection Method for Piezoelectric Touch Sensing in Noisy Environment. IEEE Sensors Journal, 2021, 21, 26373-26381.	4.7	4
33	A Fuzzy PID-Controlled Iterative Calderon's Method for Binary Distribution in Electrical Capacitance Tomography. IEEE Transactions on Instrumentation and Measurement, 2021, 70, 1-11.	4.7	9
34	MXenes: Synthesis, Optical Properties, and Applications in Ultrafast Photonics. Small, 2021, 17, e2006054.	10.0	119
35	MXenes: MXenes: Synthesis, Optical Properties, and Applications in Ultrafast Photonics (Small 11/2021). Small, 2021, 17, 2170048.	10.0	3
36	Precise wide-band electrical impedance spectroscopy measurement via an ADC operated below the Nyquist sampling rate. Measurement: Journal of the International Measurement Confederation, 2021, 174, 108995.	5.0	2

#	Article	IF	CITATIONS
37	Absolute Wavenumber Determination for Distributed Feedback Laser from Absorption Spectral Profiles. , 2021, , .		0
38	A Fractional-Order PID Controlled Iterative Calderon's Method for Electrical Capacitance Tomography. , 2021, , .		0
39	Influence of Parameters in Kalman-filter-based Method on Image Quality for Electrical Capacitance Tomography. , 2021, , .		1
40	3D Reconstruction in Planar Array Electrical Capacitance Tomography Based on Depth Estimation and Sparse Representation. , 2021, , .		2
41	Dynamic measurement of thickness distribution in a soap film by using a phase-modulated large lateral shearing interferometer. , 2021, , .		Ο
42	Online Multi-Target Laser Ranging Using Waveform Decomposition on FPGA. IEEE Sensors Journal, 2021, 21, 10879-10889.	4.7	9
43	Ultra-Low Sampled and High Precision TDLAS Thermometry Via Artificial Neural Network. IEEE Photonics Journal, 2021, 13, 1-9.	2.0	6
44	A multi-target on-line ranging method based on matrix sparsification and a division-free Gauss–Jordan solver. Measurement Science and Technology, 2021, 32, 095207.	2.6	3
45	Biomedical Applications of Electromagnetic Detection: A Brief Review. Biosensors, 2021, 11, 225.	4.7	13
46	Soft and plasmonic hydrogel optical probe for glucose monitoring. Nanophotonics, 2021, 10, 3549-3558.	6.0	23
47	Retrieval of Phase and Temperature Distributions in Axisymmetric Flames From Phase-Modulated Large Lateral Shearing Interferogram. IEEE Transactions on Instrumentation and Measurement, 2021, 70, 1-12.	4.7	7
48	Real-Time 3-D Imaging and Velocity Measurement of Two-Phase Flow Using a Twin-Plane ECT Sensor. IEEE Transactions on Instrumentation and Measurement, 2021, 70, 1-10.	4.7	14
49	An FPGA-Based On-Chip Neural Network for TDLAS Tomography in Dynamic Flames. IEEE Transactions on Instrumentation and Measurement, 2021, 70, 1-11.	4.7	15
50	3-D Image Reconstruction in Planar Array ECT by Combining Depth Estimation and Sparse Representation. IEEE Transactions on Instrumentation and Measurement, 2021, 70, 1-9.	4.7	23
51	Airborne LiDAR: state-of-the-art of system design, technology and application. Measurement Science and Technology, 2021, 32, 032002.	2.6	29
52	Flexible and Wearable EMG and PSD Sensors Enabled Locomotion Mode Recognition for IoHT-Based In-Home Rehabilitation. IEEE Sensors Journal, 2021, 21, 26311-26319.	4.7	30
53	Tissue Recognition with Deep Ensemble Learning of Ultrasound Wavelet Spectra. , 2021, , .		1
54	Parameter Inversion Based on Levenberg-Marquardt Algorithm for Layered Formation Using		1

#	Article	IF	CITATIONS
55	Temperature imaging of Counterflow Diffusion Flames by using TDLAS Tomography. , 2021, , .		2
56	RBF-based reconstruction method for tomographic imaging of temperature and water vapor concentration in flames. , 2021, , .		0
57	Quasi-Monopole Ultrasound pulse transducer based on Piezoelectric ceramic material. , 2021, , .		0
58	Corn Seedling Monitoring Using 3-D Point Cloud Data From Terrestrial Laser Scanning and Registered Camera Data. IEEE Geoscience and Remote Sensing Letters, 2020, 17, 137-141.	3.1	2
59	Effects of water vapor addition on NO reduction of <i>n</i> -decane/air flames. Energy Sources, Part A: Recovery, Utilization and Environmental Effects, 2020, 42, 1526-1540.	2.3	6
60	A new simplified mechanism for combustion of RP-3/Jet-A kerosene. Energy Sources, Part A: Recovery, Utilization and Environmental Effects, 2020, 42, 676-687.	2.3	4
61	Spectrum enhanced colour ultrasound (SECU) imaging. Measurement: Journal of the International Measurement Confederation, 2020, 154, 107401.	5.0	6
62	Dynamic measurement of gas volume fraction in a CO2 pipeline through capacitive sensing and data driven modelling. International Journal of Greenhouse Gas Control, 2020, 94, 102950.	4.6	10
63	A Compact Laser Absorption Spectroscopy Tomographic System With Short Spectral Scanning Time and Adjustable Frame Rate. IEEE Transactions on Instrumentation and Measurement, 2020, 69, 8226-8237.	4.7	24
64	A Compact Noise-Immune TDLAS Temperature Sensor using Intensity Modulation. , 2020, , .		3
65	A flexibly reconfigurable data acquisition system for tunable diode laser absorption spectroscopy. , 2020, , .		0
66	Water holdup prediction of oil-water two-phase flow in horizontal well using a 12-probe conductance array. , 2020, , .		1
67	Edge Effect Analysis and Edge Defect Detection of Titanium Alloy Based on Eddy Current Testing. Applied Sciences (Switzerland), 2020, 10, 8796.	2.5	15
68	Dynamic flashback induced by sound wave in a premixed bluff-body stabilized flame. IOP Conference Series: Earth and Environmental Science, 2020, 546, 042019.	0.3	0
69	A WMS Based TDLAS Tomographic System for Distribution Retrievals of Both Gas Concentration and Temperature in Dynamic Flames. IEEE Sensors Journal, 2020, 20, 4179-4188.	4.7	31
70	Ensemble Learning-Based Technique for Force Classifications in Piezoelectric Touch Panels. IEEE Sensors Journal, 2020, , 1-1.	4.7	3
71	Frequency-Division Multiplexing and Main Peak Scanning WMS Method for TDLAS Tomography in Flame Monitoring. IEEE Transactions on Instrumentation and Measurement, 2020, 69, 9087-9096.	4.7	56
72	Review on wavelength-tunable pulsed fiber lasers based on 2D materials. Optics and Laser Technology, 2020, 131, 106375.	4.6	39

#	Article	IF	CITATIONS
73	Online Gauss–Newton-Based Parallel-Pipeline Method for Real-Time <i>In-Situ</i> Laser Ranging. IEEE Sensors Journal, 2020, 20, 7087-7096.	4.7	11
74	A lamination-based piezoelectric insole gait analysis system for massive production for Internet-of-health things. International Journal of Distributed Sensor Networks, 2020, 16, 155014772090543.	2.2	11
75	A force–voltage responsivity stabilization method for piezoelectric-based insole gait analysis for high detection accuracy in health monitoring. International Journal of Distributed Sensor Networks, 2020, 16, 155014772090544.	2.2	9
76	A Touch Orientation Classification-Based Force–Voltage Responsivity Stabilization Method for Piezoelectric Force Sensing in Interactive Displays. IEEE Sensors Journal, 2020, 20, 8147-8154.	4.7	13
77	Solution-processed two-dimensional materials for ultrafast fiber lasers (invited). Nanophotonics, 2020, 9, 2169-2189.	6.0	43
78	A linear temperature extraction method from Voigt lineshape profile in laser absorption spectroscopy. , 2020, , .		1
79	High Security User Authentication Enabled by Piezoelectric Keystroke Dynamics and Machine Learning. IEEE Sensors Journal, 2020, 20, 13037-13046.	4.7	18
80	Inverse Radon Method Based on Electrical Field Lines for Dual-Modality Electrical Tomography. IEEE Transactions on Instrumentation and Measurement, 2020, 69, 8250-8260.	4.7	8
81	A PVDF/Au/PEN Multifunctional Flexible Human-Machine Interface for Multidimensional Sensing and Energy Harvesting for the Internet of Things. IEEE Sensors Journal, 2020, 20, 7556-7568.	4.7	27
82	Permittivity Reconstruction in Electrical Capacitance Tomography Based on Visual Representation of Deep Neural Network. IEEE Sensors Journal, 2020, 20, 4803-4815.	4.7	45
83	Lean blowout detection for bluff-body stabilized flame. Fuel, 2020, 266, 117008.	6.4	15
84	Estimation of Combustion Temperature Field From the Electrical Admittivity Distribution Obtained by Electrical Tomography. IEEE Transactions on Instrumentation and Measurement, 2020, 69, 6271-6280.	4.7	22
85	A Smart Terrain Identification Technique Based on Electromyography, Ground Reaction Force, and Machine Learning for Lower Limb Rehabilitation. Applied Sciences (Switzerland), 2020, 10, 2638.	2.5	19
86	In-vivo histocompatibility and osteogenic potential of biodegradable PLDLA composites containing silica-based bioactive glass fiber. Journal of Biomaterials Applications, 2020, 35, 59-71.	2.4	2
87	Passively Q-switched Yb-doped all-fiber laser based on Ag nanoplates as saturable absorber. Nanophotonics, 2020, 9, 3873-3880.	6.0	22
88	Suppression of reverberations at fiber tips for optical ultrasound sensing. Optics Letters, 2020, 45, 2526.	3.3	12
89	Random vibration-driven continuous-wave CRDS system for calibration-free gas concentration measurement. Optics Letters, 2020, 45, 746.	3.3	2

90 Fiber-optic ultrasound sensor with low reverberating noises. , 2020, , .

0

#	Article	IF	CITATIONS
91	Investigation of Beam Features of Unidirectional Rayleigh Waves Electromagnetic Acoustic Transducers (EMATs) by a Wholly Analytical Solution. Studies in Applied Electromagnetics and Mechanics, 2020, , .	0.2	0
92	Recent development of electromagnetic wave resistivity tools for loggingâ€whileâ€drilling. Acta Geologica Sinica, 2019, 93, 291-291.	1.4	0
93	Forward solver for deep earth exploration and induction logging using custom built Edgeâ€Element FEM technique. Acta Geologica Sinica, 2019, 93, 302-304.	1.4	3
94	A survey of underground detection methods with a new proposal for urban underground detection. Acta Geologica Sinica, 2019, 93, 322-324.	1.4	0
95	Real-Time <i>In Situ</i> Laser Ranging Based on Online Echo Waveform Fitting. IEEE Sensors Journal, 2019, 19, 9255-9262.	4.7	16
96	Effects of crustacean hyperglycemic hormone (CHH) on regulation of hemocyte intracellular signaling pathways and phagocytosis in white shrimp Litopenaeus vannamei. Fish and Shellfish Immunology, 2019, 93, 559-566.	3.6	32
97	Investigation of Multi-Plane Scheme for Compensation of Fringe Effect of Electrical Resistance Tomography Sensor. Sensors, 2019, 19, 3132.	3.8	1
98	Three-dimensional laser absorption spectroscopy velocimetry for high-speed flow diagnosis. Applied Physics B: Lasers and Optics, 2019, 125, 1.	2.2	3
99	Signal Demodulation Methods for Electrical Tomography: A Review. IEEE Sensors Journal, 2019, 19, 9026-9035.	4.7	12
100	Investigation of granule moisture measurement by a microwave resonant cavity sensor. , 2019, , .		0
101	Proportional–Integral Controller Modified Landweber Iterative Method for Image Reconstruction in Electrical Capacitance Tomography. IEEE Sensors Journal, 2019, 19, 8790-8802.	4.7	18
102	A Capacitive Information-Based Force-Voltage Responsivity Stabilization Method for Piezoelectric Touch Panels. IEEE Journal of the Electron Devices Society, 2019, 7, 1018-1025.	2.1	12
103	Fast wavelength modulated TDLAS imaging system for flame monitoring. , 2019, , .		2
104	Transcriptome analysis of hemocytes from the white shrimp Litopenaeus vannamei with the injection of dopamine. Fish and Shellfish Immunology, 2019, 94, 497-509.	3.6	21
105	Factors influencing assessment in a TDC-based ranging system. Measurement Science and Technology, 2019, 30, 125018.	2.6	2
106	Adaptive Selection of Truncation Radius in Calderon's Method for Direct Image Reconstruction in Electrical Capacitance Tomography. Sensors, 2019, 19, 2014.	3.8	3
107	Crustacean hyperglycemic hormone (CHH) affects hemocyte intracellular signaling pathways to regulate exocytosis and immune response in white shrimp Litopenaeus vannamei. Peptides, 2019, 116, 30-41.	2.4	23
108	Asymmetrical-Gaussian-Model-Based Laser Echo Detection. IEEE Sensors Journal, 2019, 19, 3797-3806.	4.7	8

#	Article	IF	CITATIONS
109	4-Dimensional Sensing in Interactive Displays Enabled by Both Capacitive and Piezoelectric Based Touch Panel. IEEE Access, 2019, 7, 33787-33794.	4.2	11
110	A robust Doppler shift-based velocimetry via using tuable diode laser absorption spectroscopy. , 2019, , \cdot		0
111	Verification for Electrical Tomography in Flame Monitoring by Ion Probe. , 2019, , .		4
112	Excitation Patterns in 3D Electrical Impedance Tomography for Breast Imaging. , 2019, , .		2
113	Improving image reconstruction in electrical capacitance tomography based on deep learning. , 2019, , .		2
114	Effect of stimulation patterns on bladder volume measurement based on fringe effect of EIT sensors. , 2019, , .		4
115	A Multi-frequency WMS Method for Tunable Diode Laser Absorption Spectroscopy Tomography. , 2019, , .		0
116	Study of Dynamic Behaviors of Thermoacoustic Oscillations by Using Laser Absorption Spectroscopy. IEEE Sensors Journal, 2019, 19, 12271-12278.	4.7	4
117	Ful1-waveform LiDAR Echo Filtering Based on Blind Source Separation. , 2019, , .		0
118	Direct Image Reconstruction for Electrical Capacitance Tomography Using Shortcut D-Bar Method. IEEE Transactions on Instrumentation and Measurement, 2019, 68, 483-492.	4.7	24
119	Automatic Registration Method for TLS LiDAR Data and Image-Based Reconstructed Data. IEEE Geoscience and Remote Sensing Letters, 2019, 16, 482-486.	3.1	1
120	An Agile Electrical Capacitance Tomography System With Improved Frame Rates. IEEE Sensors Journal, 2019, 19, 1416-1425.	4.7	16
121	Special Section on Imaging Systems and Techniques 2017. Measurement Science and Technology, 2019, 30, 020103.	2.6	0
122	Laser absorption spectroscopy for combustion diagnosis in reactive flows: A review. Applied Spectroscopy Reviews, 2019, 54, 1-44.	6.7	140
123	Reconstruction of two-dimensional velocity distribution in scramjet by laser absorption spectroscopy tomography. Applied Optics, 2019, 58, 205.	1.8	23
124	?m-resolution thickness distribution measurement of transparent glass films by using a multi-wavelength phase-shift extraction method in the large lateral shearing interferometer. Optics Express, 2019, 27, 2899.	3.4	6
125	Fiber optic-based laser interferometry array for three-dimensional ultrasound sensing. Optics Letters, 2019, 44, 5852.	3.3	15
126	Online Cross-Sectional Monitoring of a Swirling Flame Using TDLAS Tomography. IEEE Transactions on Instrumentation and Measurement, 2018, 67, 1338-1348.	4.7	79

#	Article	IF	CITATIONS
127	Particle sizing from Fraunhofer diffraction pattern using a digital micro-mirror device and a single photodiode. Powder Technology, 2018, 332, 351-358.	4.2	7
128	Prediction of equivalence ratio in pulse combustor from ion current amplitude spectrum. Fuel, 2018, 218, 179-187.	6.4	13
129	Effects of ammonia-N exposure on the concentrations of neurotransmitters, hemocyte intracellular signaling pathways and immune responses in white shrimp Litopenaeus vannamei. Fish and Shellfish Immunology, 2018, 75, 48-57.	3.6	50
130	FPCA-Based Real-Time Implementation of Temperature Measurement via Tunable Diode Laser Absorption Spectroscopy. IEEE Sensors Journal, 2018, 18, 2751-2758.	4.7	12
131	On the regularization for nonlinear tomographic absorption spectroscopy. Journal of Quantitative Spectroscopy and Radiative Transfer, 2018, 206, 233-241.	2.3	23
132	A method for compensating platform attitude fluctuation for helicopter-borne LiDAR: Performance and effectiveness. Measurement: Journal of the International Measurement Confederation, 2018, 125, 37-47.	5.0	1
133	An Iterative Algorithm Based on the Dual Integral Inversion for Particle Sizing. IEEE Transactions on Instrumentation and Measurement, 2018, 67, 1729-1737.	4.7	3
134	Special section on imaging systems and techniques 2016. Measurement Science and Technology, 2018, 29, 050101.	2.6	1
135	Eccentric Design of Fabry-Perot Interferometer for High Sensitivity and Broadband Ultrasound Sensing. , 2018, , .		0
136	Dynamic Characterization of Pulse Combustion by Image Series Processing. IEEE Sensors Journal, 2018, 18, 9682-9690.	4.7	4
137	Compensation for fringe effect of electrical resistance tomography sensor by multiple-plane sensor scheme. , 2018, , .		0
138	Color ultrasound imaging and detection technique based on nonlinear spectra. , 2018, , .		1
139	Terrestrial Laser Scanner Autonomous Self-Calibration With No Prior Knowledge of Point-Clouds. IEEE Sensors Journal, 2018, 18, 9277-9285.	4.7	16
140	Independent and simultaneous effect of crustacean hyperglycemic hormone and dopamine on the hemocyte intracellular signaling pathways and immune responses in white shrimp Litopenaeus vannamei. Fish and Shellfish Immunology, 2018, 83, 262-271.	3.6	11
141	Dual-Modality Electrical Tomography for Flame Monitoring. IEEE Sensors Journal, 2018, 18, 8847-8854.	4.7	27
142	Optimal selection of spectral lines for multispectral absorption tomography. Applied Physics B: Lasers and Optics, 2018, 124, 1.	2.2	4
143	Iterative Reconstruction Algorithm for Electrical Capacitance Tomography Based on Calderon's Method. IEEE Sensors Journal, 2018, 18, 8450-8462.	4.7	18
144	Co-path full-waveform LiDAR for detection of multiple along-path objects. Optics and Lasers in Engineering, 2018, 111, 211-221.	3.8	20

1

#	Article	IF	CITATIONS
145	A LiDAR data-based camera self-calibration method. Measurement Science and Technology, 2018, 29, 075205.	2.6	3
146	Detection of Water Leakage in Underground Tunnels Using Corrected Intensity Data and 3D Point Cloud of Terrestrial Laser Scanning. IEEE Access, 2018, 6, 32471-32480.	4.2	32
147	Lab-built terrestrial laser scanner self-calibration using mounting angle error correction. Optics Express, 2018, 26, 14444.	3.4	8
148	Influence of Waveform Characteristics on LiDAR Ranging Accuracy and Precision. Sensors, 2018, 18, 1156.	3.8	42
149	A Recursive Demodulator for Real-Time Measurement of Multiple Sinusoids. IEEE Sensors Journal, 2018, 18, 6281-6289.	4.7	8
150	Real-Time Imaging and Holdup Measurement of Carbon Dioxide Under CCS Conditions Using Electrical Capacitance Tomography. IEEE Sensors Journal, 2018, 18, 7551-7559.	4.7	17
151	A Reconfigurable Parallel Data Acquisition System for Tunable Diode Laser Absorption Spectroscopy Tomography. IEEE Sensors Journal, 2017, 17, 8215-8223.	4.7	15
152	Flame monitoring of a model swirl injector using 1D tunable diode laser absorption spectroscopy tomography. Measurement Science and Technology, 2017, 28, 054002.	2.6	27
153	Full-waveform LiDAR echo decomposition based on wavelet decomposition and particle swarm optimization. Measurement Science and Technology, 2017, 28, 045205.	2.6	16
154	A Fuzzy PID Controller-Based Two-Axis Compensation Device for Airborne Laser Scanning. IEEE Sensors Journal, 2017, 17, 1353-1362.	4.7	11
155	Support-vector-regression-based prediction of water holdup in horizontal oil-water flow by using a bicircular conductance probe array. Flow Measurement and Instrumentation, 2017, 57, 64-72.	2.0	5
156	Distribution retrieval of temperature from its histograms via the tunable diode laser absorption spectroscopy. , 2017, , .		2
157	LiDAR Ranging System Based on Automatic Gain Control and Timing Discriminators. , 2017, , .		2
158	Reconstruction of two-dimensional temperature distribution in swirling flames using TDLAS-based tomography. , 2017, , .		4
159	Point cloud acquisition using target image-aided attitude determination method. , 2017, , .		0
160	lon current sensing-based lean blowout detection for a pulse combustor. Combustion and Flame, 2017, 176, 263-271.	5.2	34
161	Ultrasonic spectral analysis for biomedical imaging. , 2017, , .		1

An image processing approach for characterizing working frequency of pulse combustion. , 2017, , .

162

#	Article	IF	CITATIONS
163	Digital Recursive Demodulator Based on Kalman Filter. IEEE Transactions on Instrumentation and Measurement, 2017, 66, 3138-3147.	4.7	21
164	Land cover classification from ICESat/GLAS waveform data. , 2017, , .		2
165	Leaf moisture content measurement using polarized active imaging LiDAR. , 2017, , .		1
166	A High-Speed Digital Electrical Capacitance Tomography System Combining Digital Recursive Demodulation and Parallel Capacitance Measurement. IEEE Sensors Journal, 2017, 17, 6690-6698.	4.7	46
167	Comparison of two approaches for land cover classification from ICESat/GLAS waveform data. , 2017, , \cdot		2
168	Terrestrial Laser Scanning Intensity Correction by Piecewise Fitting and Overlap-Driven Adjustment. Remote Sensing, 2017, 9, 1090.	4.0	32
169	Influence of Time-Pickoff Circuit Parameters on LiDAR Range Precision. Sensors, 2017, 17, 2369.	3.8	14
170	Local integrated absorbance tomography based on revised iterative reconstruction-reprojection algorithm. , 2017, , .		0
171	GPS-aided method for platform attitude determination based on target images. Applied Optics, 2017, 56, 2378.	2.1	5
172	Effects of views and spectral lines numbers on hyperspectral temperature distribution tomography. , 2016, , .		0
173	Reconstruction of temperature distribution for swirling flames using one-dimensional TDLAS tomography. , 2016, , .		0
174	Tunable diode laser absorption spectroscopy-based tomography system for on-line monitoring of two-dimensional distributions of temperature and H2O mole fraction. Review of Scientific Instruments, 2016, 87, 013101.	1.3	35
175	Water holdup measurement of oil–water two-phase flow in a horizontal well using a dual-circle conductance probe array. Measurement Science and Technology, 2016, 27, 115101.	2.6	7
176	Within-footprint roughness measurements using ICESat/GLAS waveform and LVIS elevation. Measurement Science and Technology, 2016, 27, 125012.	2.6	7
177	Identification of Oil–Water Flow Patterns in a Vertical Well Using a Dual-Ring Conductance Probe Array. IEEE Transactions on Instrumentation and Measurement, 2016, 65, 1249-1258.	4.7	25
178	Compressive sensing for particle size retrieval by using a digital micro-mirror device-based detector. Powder Technology, 2016, 304, 27-31.	4.2	3
179	Optical design of high resolution and shared aperture electro-optical/infrared sensor for UAV remote sensing applications. , 2016, , .		1
180	Surface slope and roughness measurement using ICESat/GLAS elevation and laser waveform. Measurement Science and Technology, 2016, 27, 095202.	2.6	9

#	Article	IF	CITATIONS
181	Optical design of common aperture and high resolution electro-optical/infrared system for aerial imaging applications. Proceedings of SPIE, 2016, , .	0.8	2
182	Compressive sensing-based wideband capacitance measurement with a fixed sampling rate lower than the highest exciting frequency. Measurement Science and Technology, 2016, 27, 035006.	2.6	4
183	A high success rate full-waveform lidar echo decomposition method. Measurement Science and Technology, 2016, 27, 015205.	2.6	19
184	A chemi-ionization processing approach for characterizing flame flickering behavior. , 2015, , .		5
185	A simplified PIV-based method for flame velocity distribution measurement. , 2015, , .		0
186	A noncontact conductivity detection method based on the principle of electromagnetic induction. , 2015, , .		0
187	Identification of oil-water flow patterns using conductance probe in vertical well. , 2015, , .		1
188	Comparative study of regression modeling methods for online coal calorific value prediction from flame radiation features. Fuel, 2015, 142, 164-172.	6.4	17
189	Performance analysis of a digital capacitance measuring circuit. Review of Scientific Instruments, 2015, 86, 054703.	1.3	62
190	Digital micro-mirror device-based detector for particle-sizing instruments via Fraunhofer diffraction. Applied Optics, 2015, 54, 5842.	2.1	7
191	Development of a fan-beam TDLAS-based tomographic sensor for rapid imaging of temperature and gas concentration. Optics Express, 2015, 23, 22494.	3.4	104
192	Water cut measurement of oil–water flow in vertical well by combining total flow rate and the response of a conductance probe. Measurement Science and Technology, 2015, 26, 095306.	2.6	8
193	Resolution-doubled one-dimensional wavelength modulation spectroscopy tomography for flame flatness validation of a flat-flame burner. Applied Physics B: Lasers and Optics, 2015, 120, 407-416.	2.2	36
194	Ghost imaging of binary-valued objects by using a CCD and an equivalent photodiode. , 2015, , .		0
195	Online Estimation of Coal Calorific Value from Combustion Radiation for Coal-Fired Boilers. Combustion Science and Technology, 2015, 187, 1487-1503.	2.3	7
196	Control Pulse Combination-Based Analysis of Pulse Train Controlled DCM Switching DC–DC Converters. IEEE Transactions on Industrial Electronics, 2015, 62, 246-255.	7.9	40
197	Bidirectional reflectance distribution function based surface modeling of non-Lambertian using intensity data of light detection and ranging. Journal of the Optical Society of America A: Optics and Image Science, and Vision, 2014, 31, 2055.	1.5	11
198	A high-speed electrical impedance measurement circuit based on information-filtering demodulation. Measurement Science and Technology, 2014, 25, 075010.	2.6	26

#	Article	IF	CITATIONS
199	Modified Landweber algorithm for robust particle sizing by using Fraunhofer diffraction. Applied Optics, 2014, 53, 6185.	1.8	14
200	Projective rectification of infrared images from air-cooled condenser temperature measurement by using projection profile features and cross-ratio invariability. Applied Optics, 2014, 53, 6482.	1.8	1
201	Digital signal processor-based high-precision on-line Voigt lineshape fitting for direct absorption spectroscopy. Review of Scientific Instruments, 2014, 85, 123108.	1.3	14
202	Reconstruction of Axisymmetric Temperature and Gas Concentration Distributions by Combining Fan-Beam TDLAS With Onion-Peeling Deconvolution. IEEE Transactions on Instrumentation and Measurement, 2014, 63, 3067-3075.	4.7	68
203	Manchester code telemetry system for well logging using quasi-parallel inductive-capacitive resonance. Review of Scientific Instruments, 2014, 85, 074704.	1.3	6
204	Factorization method for electrical resistance tomography with partial boundary measurements. , 2014, , .		1
205	A digital demodulator based on the recursive Gauss-Newton method for electrical tomography. , 2014, , ,		2
206	One-dimensional tomography of axisymmetric temperature distribution with limited TDLAS data by using three-point Abel deconvolution. , 2014, , .		0
207	A high precision method for mapping phase to amplitude in direct digital synthesis and its hardware implementation. Review of Scientific Instruments, 2014, 85, 114704.	1.3	2
208	Multiple parameters× ³ estimation in horizontal well logging using a conductance-probe array. Flow Measurement and Instrumentation, 2014, 40, 192-198.	2.0	21
209	A novel full-waveform LiDAR echo decomposition method and simulation verification. , 2014, , .		2
210	Four-Terminal Imaging Using a Two-Terminal Electrical Impedance Tomography System. IEEE Transactions on Instrumentation and Measurement, 2014, 63, 432-440.	4.7	22
211	K-Plane-Based Classification of Airborne LiDAR Data for Accurate Building Roof Measurement. IEEE Transactions on Instrumentation and Measurement, 2014, 63, 1200-1214.	4.7	39
212	Coil shape optimization of the electromagnetic flowmeter for different flow profiles. Flow Measurement and Instrumentation, 2014, 40, 256-262.	2.0	18
213	Real-time terrain classification using ICESat/GLAS data over Beijing area. Remote Sensing Letters, 2014, 5, 591-600.	1.4	5
214	On-the-Fly Extraction of Polyhedral Buildings From Airborne LiDAR Data. IEEE Geoscience and Remote Sensing Letters, 2014, 11, 1946-1950.	3.1	13
215	Analysis of the electromagnetic wave resistivity tool in deviated well drilling. , 2014, , .		0
216	Comparative study of computational intelligence approaches for NOx reduction of coal-fired boiler. Energy, 2013, 55, 683-692.	8.8	58

#	Article	IF	CITATIONS
217	A Proposal to Compensate Platform Attitude Deviation's Impact on Laser Point Cloud From Airborne LiDAR. IEEE Transactions on Instrumentation and Measurement, 2013, 62, 2549-2558.	4.7	11
218	Land classification from LiDAR full-waveforms based on multi-class support vector machines. , 2013, , .		2
219	Laser spot center location by using the gradient-based and least square algorithms. , 2013, , .		4
220	Direct image reconstruction for ERT by using measurements on partial boundary. , 2013, , .		3
221	Impact of attitude measurement errors on laser footprints positioning accuracy. , 2013, , .		1
222	Optimization of the Electromagnetic Wave Resistivity tool in Logging While Drilling. , 2013, , .		1
223	A Digital Switching Demodulator for Electrical Capacitance Tomography. IEEE Transactions on Instrumentation and Measurement, 2013, 62, 1025-1033.	4.7	38
224	Direct Image Reconstruction for 3-D Electrical Resistance Tomography by Using the Factorization Method and Electrodes on a Single Plane. IEEE Transactions on Instrumentation and Measurement, 2013, 62, 999-1007.	4.7	19
225	A federal UKF algorithm in INS/GPS/aerial image integrated attitude determination system. , 2013, , .		1
226	Determination of platform attitude through SURF based aerial image matching. , 2013, , .		2
227	Dew point measurement using a quartz crystal sensor. , 2013, , .		2
228	Measurement of axisymmetric temperature distributions using single view fan-beam TDLAS tomography. , 2013, , .		3
229	Particle size influence on effective permittivity of particle–gas mixture with particle clusters. Particuology, 2013, 11, 216-224.	3.6	7
230	Identification of amino acids responsible for stop codon recognition for polypeptide chain release factor. Biochemistry and Cell Biology, 2013, 91, 155-164.	2.0	1
231	Measurement of nonuniform temperature and concentration distributions by combining line-of-sight tunable diode laser absorption spectroscopy with regularization methods. Applied Optics, 2013, 52, 4827.	1.8	56
232	Empirical modeling for non-Lambertian reflectance based on full-waveform laser detection. Optical Engineering, 2013, 52, 116110.	1.0	13
233	A recursive least squares-based demodulator for electrical tomography. Review of Scientific Instruments, 2013, 84, 044704.	1.3	19
234	A complex programmable logic device-based high-precision electrical capacitance tomography system. Measurement Science and Technology, 2013, 24, 074006.	2.6	16

#	Article	IF	CITATIONS
235	Direct recovery of the electrical admittivities in 2D electrical tomography by using Calderon's method and two-terminal/electrode excitation strategies. Measurement Science and Technology, 2013, 24, 074007.	2.6	18
236	A new method for building roof segmentation from airborne LiDAR point cloud data. Measurement Science and Technology, 2013, 24, 095402.	2.6	20
237	A real-time method for DSM generation from airborne LiDAR data. , 2013, , .		8
238	Quantitatively Evaluating Random Attitude Measurement Errors' Impacts on DSM Elevation Accuracy From Airborne Laser Scanning. IEEE Transactions on Instrumentation and Measurement, 2013, 62, 3101-3109.	4.7	11
239	Full-waveform LiDAR signal filtering based on Empirical Mode Decomposition method. , 2013, , .		5
240	An automatic algorithm for slope estimation from repeat tracks of ICESat/GLAS. , 2013, , .		0
241	2D image reconstruction of a human chest by using Calderon's method and the adjacent current pattern. Journal of Instrumentation, 2013, 8, P03004-P03004.	1.2	13
242	Direct image reconstruction for 3D electrical resistance tomography by using the factorization method. , 2012, , .		4
243	Terrain slope calculation from waveform of airborne LiDAR. , 2012, , .		1
244	Projective rectification of infrared image based on projective geometry. , 2012, , .		0
245	Influence of installation angle of electromagnetic flowmeter on measurement accuracy. , 2012, , .		1
246	Slope estimations in forest area from waveform and DEM. , 2012, , .		0
247	Simulation of double closed-loop FLC for the compensating platform of LiDAR. , 2012, , .		0
248	Normalized least-square method for water hold-up measurement in stratified oil–water flow. Flow Measurement and Instrumentation, 2012, 27, 71-80.	2.0	23
249	Measurement of airborne platform attitude by using aerial images. , 2012, , .		0
250	A kernel-density-estimation-based outlier detection for airborne LiDAR point clouds. , 2012, , .		1
251	A new concept for the distributions of wavelet packet decomposition coefficients in detail subbands. , 2012, , .		0
252	An adaptive algorithm for cross-correlation velocity measurement. , 2012, , .		5

#	Article	IF	CITATIONS
253	Simulation on measuring of nonuniform temperature distribution based on line-of-sight TDLAS by using Tikhonov regularization method. , 2012, , .		1
254	Fan-beam TDLAS tomography for gas concentration distribution with limited data. , 2012, , .		0
255	Effect of inclined angle of fuel jet on NO <inf>x</inf> emission in high temperature air combustion. , 2012, , .		1
256	Optimization of Operating Parameters for Low NO _{<i>x</i>} Emission in High-Temperature Air Combustion. Energy & Fuels, 2012, 26, 2821-2829.	5.1	22
257	Independent Component Analysis–Based Fuel Type Identification for Coal-Fired Power Plants. Combustion Science and Technology, 2012, 184, 277-292.	2.3	9
258	Estimation of cluster centers on building roof from LiDAR footprints. , 2012, , .		4
259	A direct reconstruction algorithm for recovering the admittivities in 2D electrical tomography. , 2012, , .		0
260	Terrain slope estimation within footprint from ICESat/GLAS waveform: model and method. Journal of Applied Remote Sensing, 2012, 6, 063534.	1.3	10
261	Image Reconstruction for Invasive ERT in Vertical Oil Well Logging. Chinese Journal of Chemical Engineering, 2012, 20, 319-328.	3.5	11
262	Fuel-Type Identification Using Joint Probability Density Arbiter and Soft-Computing Techniques. IEEE Transactions on Instrumentation and Measurement, 2012, 61, 286-296.	4.7	15
263	Quantitative Evaluation of Impacts of Random Errors on ALS Accuracy Using Multiple Linear Regression Method. IEEE Transactions on Instrumentation and Measurement, 2012, 61, 2242-2252.	4.7	15
264	\$ell_{1}\$-Norm-Based Reconstruction Algorithm for Particle Sizing. IEEE Transactions on Instrumentation and Measurement, 2012, 61, 1395-1404.	4.7	17
265	Direct image reconstruction for electromagnetic tomography by using the factorization method. , 2011, , .		0
266	A simplified model for non-destructive thickness measurement immune to the lift-off effect. , 2011, , .		1
267	Compensation of optical path difference for colorimetric temperature imaging. , 2011, , .		0
268	Design on the aerial survey parameters of the airborne LiDAR. , 2011, , .		2
269	Model of measuring slop from raw data of full-waveform topographic lidar. , 2011, , .		0
270	Weighting function-based coil size optimization for electromagnetic flowmeter. , 2011, , .		2

#	Article	IF	CITATIONS
271	Simulation on impact of random attitude measurement errors on point cloud and 3D image of ALS. , 2011, , .		6
272	DC bias compensation in digital AC-based capacitance measurement for ECT. , 2011, , .		1
273	FPGA-based implementation of Prony demodulation in the multi-frequency EIT system. , 2011, , .		1
274	Electrical Capacitance Tomography for Sensors of Square Cross Sections Using Calderon's Method. IEEE Transactions on Instrumentation and Measurement, 2011, 60, 900-907.	4.7	56
275	Wet Gas Metering Using a Revised Venturi Meter and Soft-Computing Approximation Techniques. IEEE Transactions on Instrumentation and Measurement, 2011, 60, 947-956.	4.7	46
276	Wet-Gas Flow Modeling for the Straight Section of Throat-Extended Venturi Meter. IEEE Transactions on Instrumentation and Measurement, 2011, 60, 2080-2087.	4.7	25
277	CFD modelling of velocity distribution in tangential coal-fired flame. , 2011, , .		Ο
278	Four-terminal scheme used in a two-terminal EIT system. , 2011, , .		3
279	Direct image reconstruction for electromagnetic tomography(EMT) by using the dbar method. , 2011, , .		2
280	ℓ <inf>1</inf> Norm based reconstruction algorithm for particle sizing. , 2011, , .		3
281	2D electrical capacitance tomography with sensors of non-circular cross sections using the factorization method. Measurement Science and Technology, 2011, 22, 114003.	2.6	8
282	Direct image reconstruction for electrical capacitance tomography by using the enclosure method. Measurement Science and Technology, 2011, 22, 104001.	2.6	18
283	Impact analysis of random measurement errors on airborne laser scanning accuracy. , 2011, , .		3
284	Electrical capacitance tomography with a non-circular sensor using the dbar method. Measurement Science and Technology, 2010, 21, 015502.	2.6	38
285	On-line identification of new coal type using joint probability density arbiter. , 2010, , .		0
286	2D ECT for sensors of non-circular cross sections using the factorization method. , 2010, , .		1
287	Real-time measurement of aerodynamic deformation of wing by laser rangefinder. , 2010, , .		2
288	A direct reconstruction method of electromagnetic tomography(EMT) for high permeability and low conductivity distributions. , 2010, , .		2

#	Article	IF	CITATIONS
289	Geometric distortion correction for sinusoidally scanned atomic force microscopic images. , 2010, , .		3
290	Wet gas flow modeling for the straight section of throat-extended Venturi meter. , 2010, , .		1
291	Electrical resistance tomography(ERT) by using an ECT sensor. , 2010, , .		5
292	On-line identification of fuel type using joint probability density arbiter and support vector machine techniques. , 2010, , .		3
293	2D ECT with square sensor using Calderon's method. , 2009, , .		0
294	Wet gas metering using a Venturi-meter and Support Vector Machines. , 2009, , .		3
295	A new analytical inversion to Fraunhofer diffraction. , 2009, , .		0
296	On-line fuel identification using optical sensing and Support Vector Machines technique. , 2009, , .		4
297	Image reconstruction technique of electrical capacitance tomography for low-contrast dielectrics using Calderon's method. Measurement Science and Technology, 2009, 20, 104027.	2.6	46
298	Integral inversion to Fraunhofer diffraction for particle sizing. Applied Optics, 2009, 48, 4842.	2.1	18
299	Experimental study on cylindrical capacitance sensor. , 2009, , .		1
300	A new cylindrical capacitance sensor for measurement of water cut in a low-production horizontal well. Journal of Physics: Conference Series, 2009, 147, 012002.	0.4	3
301	Dual-Channel Pseudorandom Sequence Generator With Precise Time Delay Between Its Two Channels. IEEE Transactions on Instrumentation and Measurement, 2008, 57, 2880-2884.	4.7	8
302	Two-in-One Implementation of Noise Reduction and Incline Emendation for Atomic Force Microscopic Images. , 2008, , .		0
303	Wet Gas Metering Using a Venturi-meter and Neural Networks. , 2008, , .		5
304	Electrical impedance tomography with an optimized calculable square sensor. Review of Scientific Instruments, 2008, 79, 103710.	1.3	30
305	Particle Size Influence on Effective Permittivity of Particle-Gas Mixture with Particles Agglomeration: Experimental Study. Conference Record - IEEE Instrumentation and Measurement Technology Conference, 2007, , .	0.0	1
306	Simultaneous Removal of Harmonic Interference and White Noise by Combining Multi-Rate Signal Processing and Wavelet Denoising Techniques. , 2007, , .		0

#	Article	IF	CITATIONS
307	An Improved Algorithm for the Measurement of Flame Oscillation Frequency. IEEE Transactions on Instrumentation and Measurement, 2007, 56, 2087-2093.	4.7	20
308	Wavelet-based removal of sinusoidal interference from a signal. Measurement Science and Technology, 2004, 15, 1779-1786.	2.6	23
309	Identification of two-phase flow regimes in horizontal, inclined and vertical pipes. Measurement Science and Technology, 2001, 12, 1069-1075.	2.6	54
310	Capacitance-based concentration measurement for gas-particle system with low particles loading. Flow Measurement and Instrumentation, 2000, 11, 185-194.	2.0	12
311	Application of ultrasonic tomography to monitoring gas/liquid flow. Chemical Engineering Science, 1997, 52, 2171-2183.	3.8	86